

Composite biomolecule/PEDOT materials for neural electrodes

Maria Asplund^{a)}

School of Technology and Health, Royal Institute of Technology, Alfred Nobels Allé 10, SE-14152 Huddinge, Sweden

Hans von Holst

School of Technology and Health, Royal Institute of Technology, Alfred Nobels Allé 10, SE-14152 Huddinge, Sweden and Institution of Laboratory Medicine, Karolinska Institutet, and Department of Neurosurgery, Karolinska University Hospital, SE-141 86 Stockholm, Sweden

Olle Inganäs

Biomolecular and Organic Electronics, The Department of Physics, Chemistry and Biology, Linköping University, SE-581 83 Linköping, Sweden

(Received 21 July 2008; accepted 10 September 2008; published 10 November 2008)

Electrodes intended for neural communication must be designed to meet both the electrochemical and biological requirements essential for long term functionality. Metallic electrode materials have been found inadequate to meet these requirements and therefore conducting polymers for neural electrodes have emerged as a field of interest. One clear advantage with polymer electrodes is the possibility to tailor the material to have optimal biomechanical and chemical properties for certain applications. To identify and evaluate new materials for neural communication electrodes, three charged biomolecules, fibrinogen, hyaluronic acid (HA), and heparin are used as counterions in the electrochemical polymerization of poly(3,4-ethylenedioxythiophene) (PEDOT). The resulting material is evaluated electrochemically and the amount of exposed biomolecule on the surface is quantified. PEDOT:biomolecule surfaces are also studied with static contact angle measurements as well as scanning electron microscopy and compared to surfaces of PEDOT electrochemically deposited with surfactant counterion polystyrene sulphonate (PSS). Electrochemical measurements show that PEDOT:heparin and PEDOT:HA, both have the electrochemical properties required for neural electrodes, and PEDOT:heparin also compares well to PEDOT:PSS. PEDOT:fibrinogen is found less suitable as neural electrode material. © 2008 American Vacuum Society.

[DOI: 10.1116/1.2998407]

I. INTRODUCTION

Electrodes artificially stimulating the nervous system are a powerful tool in the treatment of several diseases and traumatic conditions. The use of electrical signals to restore and replace lost body function has already proven a successful strategy in several applications such as the cochlear implant and deep brain stimulation and within the field of neuroprosthetics, extensive effort is placed into widening the span of applications for such electrode systems.

The key element in a neuroprosthetic system is the electrode/electrolyte interface which is the component translating signals from electronic form to ionic form, allowing transmission to target neural tissue, through ionic conduction in body fluids. A prerequisite for most neuroprosthetic systems is that stimulation and recording can be done selectively on smaller populations of neurons, which in turn mean that electrodes preferably should be implanted in proximity to the target tissue.

One of the main inhibitors of neural controlled prosthesis and artificial sensing today is the lack of electrode materials suitable for prolonged implantation and stimulation. Not only must every requirement of biocompatibility and biostability of the system be met, but it is of the utmost importance

that pulses are kept within the electrochemical safety levels implied both by the electrode material and surrounding body fluids.^{1,2} Further, many applications are depending on a high number of individual electrodes to be implanted and miniaturization of these systems are therefore necessary. Higher electrode density increase possibility to stimulate selectively³ and also most neural implants must be fitted into very restricted spaces.

However, there is a conflict between miniaturized electrodes on one hand and high charge delivery on the other hand since most electronic to ionic transmissions are depending on capacitance at the electrode/electrolyte interface, implying a maximum reversible charge delivery proportional to electrode area. Finding materials allowing sufficient charge delivery from small electrodes is therefore an important step toward more sophisticated neuroprosthetic systems. Another point of attack would be to enable closer contact between electrode and target neuron, minimizing the signal needed to elicit the desired response.

Rapid progress within the field of organic electronics have lead to the development of stable conducting polymers possible to use within a wide set of applications including medical devices. The conducting polymer poly(3,4-ethylene dioxathiophene) (PEDOT) has emerged as an interesting candidate for neuroelectronic interfaces, based on its excel-

^{a)}Electronic mail: maria.asplund@sth.kth.se

lent conductivity and stability properties and indications on its good compatibility with biological structures.⁴⁻⁶ PEDOT coatings have been shown to lower interfacial impedance on recording electrodes by several orders of magnitude^{4,7,8} and increase charge delivery capacity through its hybrid charge transfer properties involving both electronic and ionic conduction.⁵ The active surface area of PEDOT coatings can also be increased further through swelling into highly porous hydrogel electrodes permeable to electrolytes, thereby significantly increasing its charge storage and delivery capacity.⁹ Nyberg *et al.*⁴ reported hydrogel PEDOT electrodes with charge delivery capacities up to 0.34 mC/mm², which clearly exceed reported levels of state of the art activated iridium oxide film electrodes at ~0.1 mC/mm².¹⁰ Furthermore, polymer coatings provide excellent opportunities to incorporate bioactive species into the electrode material itself, both for active and passive drug deliveries, implying that polymer electrodes can be useful both for improving charge delivery capacity and also biochemically encourage closer contact with target nervous tissue.⁶ The softness of the polymer film is also believed to increase the chances of prolonged neuronal contact,⁴ in contrast to hard metallic surfaces.

PEDOT can be electrosynthesized from aqueous solutions containing different kinds of doping anions. A common choice is polystyrene sulphonate (PSS), which due to its surfactant properties have been found to facilitate electropolymerization.^{11,12} The use of PSS is well established when working with PEDOT in organic electronics, but might on the other hand not be the best choice for creating a friendly environment for neural cells, considering its acidic and surfactant properties. Although it has been shown that cells can be cultured on top of PEDOT:PSS substrates,¹³ the aim must be not just to ensure cell survival but actually encourage them to grow on the electrode material. Other ions, surfactants,^{12,14,15} or nonsurfactants^{11,13,16} can be chosen instead of PSS as counterion, and can be tailored to provide optimal conditions for implanted electrodes. Body fluids contain many ions of low molecular weight that can be used as counterions in the electropolymerization of PEDOT. The ionic conductance of PEDOT films does however partly depend on the counterion used in polymerization, and smaller ions tend to create PEDOT coatings with limited possibilities for conduction of larger ionic species.¹¹ If possible, larger counterions would therefore be preferable. It has previously been demonstrated that polypyrrole (PPy) can be deposited using peptides or proteins as counterions¹⁷ and PEDOT has been polymerized from peptides in acetonitrile solvent¹⁸ and PEDOT-MeOH from peptide solution.⁶ We believe a similar strategy should be applicable for a large selection of biomolecules using only aqueous solution and EDOT monomer.

To identify and evaluate new materials for neural electrodes, three charged biomolecules, fibrinogen, hyaluronic acid (HA), and heparin, have been paired with PEDOT as counterions in electropolymerization. These biomolecules are already present in abundance in tissue and are commer-

cially available in larger quantities. HA is a glucosaminoglycan and an important component of the extracellular matrix also in neural tissue and has been found to enhance peripheral nerve regeneration. Heparin is a polysaccharide mainly known for its anticoagulant properties and to provide very hydrophilic surface coatings. Fibrinogen is a protein with a central role in the mechanism of coagulation and thrombosis. Previous studies have investigated PPy surfaces functionalized with immobilized HA¹⁹ and heparin²⁰ as interesting substrates for tissue engineering and also successfully electropolymerized PPy with heparin^{21,22} or HA as counterion.²³ Here we show that it is possible to electropolymerize EDOT from aqueous solutions with these biomolecules as counterions, and also a large protein such as fibrinogen can be used. Cyclic voltammetry measurements confirmed that the amount of electroactive polymer deposited can be controlled by varying deposition charge as known for polymerization with other counterions. The toluidine blue assay was used to confirm that heparin and HA was incorporated in the polymer films and isotope staining (iodine-125) was used for the detection of fibrinogen. Films were analyzed further with both electrical impedance spectroscopy (EIS), scanning electron microscopy (SEM) and with contact angle measurements to study their wettability and surface roughness.

II. MATERIALS AND METHODS

Heparin sodium salt from porcine intestinal mucosa (202 units/mg) was purchased from Sigma-Aldrich, hyaluronic acid sodium salt from streptococcus equi was purchased from Fluka Biochemica, and fibrinogen obtained from citrated human plasma was purchased from Hyphen BioMed. Poly(NaPSS) (MW CA 70000) was purchased from Aldrich. EDOT (Bayer AG) was dissolved in milli-Q water (purified to 18 MΩ cm⁻²) at a concentration of 0.01M through an ultrasonic bath and subsequent stirring for at least 1 h. From this solution, three biomolecule solutions with 0.01M EDOT were prepared; 5 mg/ml heparin, 5 mg/ml fibrinogen, 1 mg/ml HA, and one solution with 5 mg/ml NaPSS. When incorporated into a neutral aqueous solution HA forms hydrogen bonds which leads to highly viscous solutions and this is the reason why a lower concentration of HA was chosen.

Polymerization, potentiometric recordings and cyclic voltammetry were performed using Autolab General Purpose Electrochemical system (GPES) and Autolab Frequency Response Analysis (FRA) system for impedance spectroscopy. All experiments were performed in a standard three electrode setup using a glassy carbon disk counterelectrode, an Ag:AgCl reference electrode and a platinum disk (2 mm²) as working electrode; all purchased from Bioanalytical Systems Inc. Prior to polymerization, working and counterelectrode were polished with aluminum oxide (0.3 μm) and rinsed with de-ionized water.

It is generally accepted that the amount of polymer built through electrochemical deposition is proportional to charge injected in the polymerization process and galvanostatic polymerization is therefore a convenient way to control the

amount of electroactive material on the electrode. Current density should be set high enough to give stable polymerization without the risk of overoxidation of already deposited layers, and a current density of 0.2 mA/cm^2 should fulfill these requirements.²⁴ A steady current of $4 \mu\text{A}$ and varying deposition time in the range 100–2000 s was therefore chosen to grow polymer layers of different thicknesses. Two samples of each PEDOT:biomolecular composite was prepared at each data point and the formed polymer was investigated with cyclic voltammetry (CV) swept from -0.5 to 0.5 V at a rate of 0.1 V/s . Polymer electrodes deposited with 1.6 mC/mm^2 were also subject to voltage pulsing to probe their current-time response. Pulse trains of 0.5 V cathodic pulses of 50 ms duration and a zero voltage intermediate interval of 200 ms were used and the resulting current response was analyzed as the average of the response of ten individual pulses.

EIS was used to study each polymer film in the interval 3 Hz – 10 kHz for a sinusoidal signal of amplitude 10 mV at a bias of 0.2 V . Polymer films deposited with 0.6 , 1.0 , 1.6 , and 2.0 mC/mm^2 for PEDOT:PSS, HA, and heparin, respectively, and for PEDOT:fibrinogen at 0.4 , 0.8 , 1.4 , and 1.8 mC/mm^2 deposited on top of a 0.2 mC/mm^2 PEDOT:NaCl-layer were investigated. Both CV and EIS were performed in 0.1 M KCl , if not stated otherwise, purged with nitrogen for at least 15 min before measurements and in a homemade Faradays' cage. Prior to EIS, polymer films were conditioned through 20 sweeps of cyclic voltammetry and when studying the same polymer films in KCl and NaPSS, films were first measured upon in KCl, then conditioned with 20 sweeps in NaPSS before measurement. EIS data were fitted with equivalent circuits using AUTOLAB FRA software.

The presence of heparin or HA in the polymer was confirmed through measuring the extraction of toluidine blue from aqueous solution as described by others.^{19,21,22,25,26} Toluidine blue is a metachromic dye that produces colored precipitates with heparin and HA. This can be quantified through measuring absorbance at 631 nm of solution which is reversely proportional to the loss of dye and thereby concentration of heparin or HA. Toluidine blue (Sigma-Aldrich) solution was dissolved, 16 mg to a 100 ml with 0.2% (w/v) NaCl and 0.01 M HCl for the heparin assay. It should be noted that toluidine blue does not give precipitate with HA at pH lower than 3.3 ²⁷ and therefore a separate toluidine blue solution with pH 4 was prepared for this purpose. Standard curves of solution absorbance were obtained through mixing 0.4 ml water of known concentration of biomolecule with 0.6 ml toluidine blue solution. After mixing, 0.6 ml n -hexane was added and solution was shaken vigorously so that precipitate was extracted into the organic layer. Absorbance of the aqueous phase was measured using 10 mm quartz cuvettes at a Perkin Elmer spectrophotometer $\lambda 9$. A linear relationship between absorbance and biomolecule concentration was determined in the concentration range 10 – $100 \mu\text{g/ml}$. For measurement on polymer layers, platinum electrodes with electrodeposited PEDOT:biomolecule

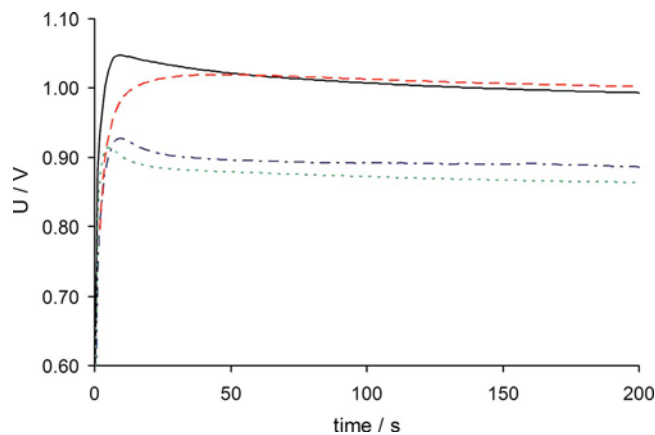


FIG. 1. Chronopotentiometric recording during galvanostatic polymerization of EDOT in aqueous solution with different biomolecular counterions, shown as follows: heparin 5 mg/ml (\cdots), HA 1 mg/ml ($-\ -$), fibrinogen 1 mg/ml (\longrightarrow), and NaPSS 5 mg/ml (\cdots).

layers were soaked in 0.4 ml water mixed with 0.6 ml toluidine blue solution for 40 min and shaken with n -hexane as described above. The incorporation of fibrinogen was confirmed through staining fibrinogen with iodine-125 and measure activity of gold electrodes coated with PEDOT:fibrinogen, on a Cobra II Auto-Gamma reader.

For the study of surface wettability and roughness, electrodes with larger surface area were prepared through the evaporation of gold (2 k\AA) on top of chrome (25 \AA) on glass through a shadow mask and polymer was deposited electrochemically with 1.8 mC/mm^2 . Such probes were also used for the iodine-125 assays. On some samples, gold was sputtered on top of the electrodeposited PEDOT films to enable the use of SEM to study the surfaces microstructure.

III. RESULTS

Galvanostatic polymerization was successful from both EDOT:heparin and EDOT:HA solutions and layers with the characteristic deep blue color of PEDOT was grown over the full interval 0.2 – 4 mC/mm^2 . From chronopotentiometric recordings (Fig. 1) during the process it could be seen that all polymerizations took place in a similar manner although required potential varied slightly between samples. Voltage initially increased until a peak, here denoted u_{max} , and was then lowered to a steady state, u_{ss} , for the remaining deposition time. Details of the polymerization for each counterion can be found in Table I and sample curves can be seen in Fig. 1.

TABLE I. Voltage recorded during galvanostatic polymerization of EDOT at 0.2 mA/cm^2 with different biomolecular counterions (average from more than 20 measurements for each counterion).

Counterion	\bar{u}_{max} (V)	\bar{u}_{ss} (V)
EDOT:HA	$1.06, \sigma=0.029$	$1.00, \sigma=0.041$
EDOT:heparin	$0.916, \sigma=0.019$	$0.872, \sigma=0.021$
EDOT:PSS	$0.916, \sigma=0.026$	$0.874, \sigma=0.037$
EDOT:fibrinogen	$1.02, \sigma=0.048$	$0.999, \sigma=0.050$

In general, polymerization took place at lower voltage for heparin solution than for HA or fibrinogen. From previous studies, low oxidation potential is expected when Na:PSS is used as supporting electrolyte. This is believed to be a consequence of the surfactant properties of PSS⁻ facilitating solubilization of the hydrophobic EDOT, as has been observed for surfactant anions by others.^{11,12,14} Interestingly, heparin as counterion gave oxidation potential similar to that of NaPSS and polymer films could be grown reliably over the full interval. Polymerization from EDOT:fibrinogen solutions was however problematic. In most cases, voltage never reached steady state but continued to increase indicating that a nonconducting layer of some kind was formed, blocking the surface. In these cases we could also not observe any blue polymer formation on the surface. Sometimes, polymerization did however start off in a similar manner as for the other electrolytes, and could continue in the same manner as observed for the other counterions.

Fibrinogen is known to quickly adhere and bind tightly to metal surfaces in continuous layers.^{28–30} It is therefore not surprising that a platinum electrode lowered in a fibrinogen solution of concentration 1 mg/ml is quickly blocked by adsorbed proteins, efficiently insulating the surface. Several paths to impede fibrinogen adsorption on to the surface were tried out, e.g., pretreating the surface with oxygen plasma, allowing the solution to age for a week to make the fibrinogen less active, or ensuring that surface was positively biased at all times in solution since fibrinogen has been shown to adhere slower and with lower coverage on positively charged platinum surfaces.²⁹ Despite these efforts, consistent polymer growth could not be achieved and we therefore decided to polymerize on a surface with less affinity for fibrinogen, i.e., not a metal surface, and to lower fibrinogen concentration from the initial 5 to 1 mg/ml. The platinum surface was first galvanostatically coated with PEDOT from 0.01M EDOT aqueous solution in a 5 mg/ml supporting NaCl electrolyte (100 s, 4 μ A). On condition that surface was positively biased at all times in fibrinogen solution, polymer with deposition charges up to 2 mC/mm² could successfully be grown from the EDOT/fibrinogen solution on top of the PEDOT:NaCl polymer. It was crucial that the polymerization process started immediately when surface was lowered in water for the surface not to be blocked. It should however be noted that the measurements obtained for these coatings describe the PEDOT/NaCl/PEDOT/fibrinogen as a complex and PEDOT/fibrinogen coatings could therefore not be analyzed as a stand alone material.

Cyclic voltammograms revealed no clear oxidation or reduction peaks over the interval -0.5 to 0.5 V, and a highly capacitive behavior was confirmed for all polymer films (Fig. 2). The area enveloped by the sweep of the CV curve, Q_{CV} , is proportional to the amount of electroactive polymer deposited and can also be used as a measure of charge storage capacity of the electrode.³¹ CV curves were therefore integrated with respect to voltage over the cathodic sweep and normalized by sweep rate 0.1 V/s, yielding Q_{CV} . A consistent growth of electroactive polymer over time should yield a

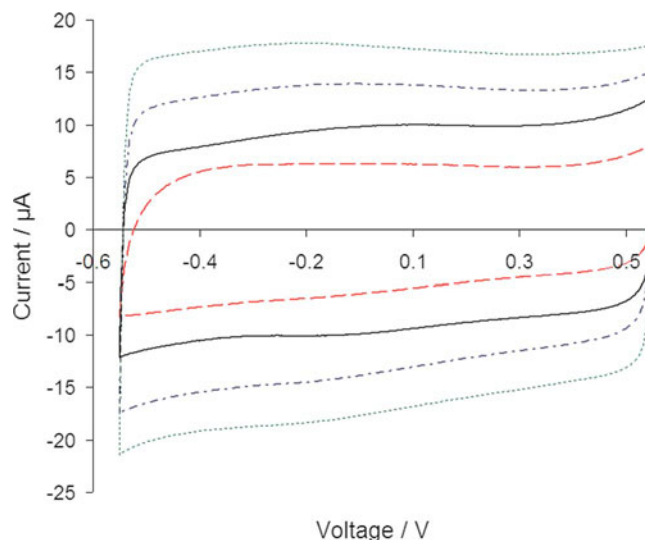


Fig. 2. Cyclic voltammograms of PEDOT film deposited with 1.6 mC/mm² with different biomolecular counterions, shown as follows: heparin 5 mg/ml shown in blue (- - -), HA 1 mg/ml shown in black (—), fibrinogen 1 mg/ml shown in red (- - -), and NaPSS 5 mg/ml shown in green (···).

linear relationship between area of the cyclic voltammogram and deposition charge. This is also confirmed by data (Fig. 3), where Q_{CV} was found to increase proportional to applied deposition charge for all four counterions, which is in good agreement with previous studies.^{4,11} Maximum deposition charge studied for PEDOT:heparin and PEDOT:HA was 4 mC/mm² (deposition time, 2000 s) but there is no reason to believe this should be considered an upper limit. We observed however that very thick polymer layers more easily delaminated from the underlying surface and had to be handled with care. For fibrinogen we did experience difficulties with growing thicker films, presumably because the conductivity of the PEDOT:fibrinogen polymer was lower, and therefore too thick layers seemed to build a barrier requiring

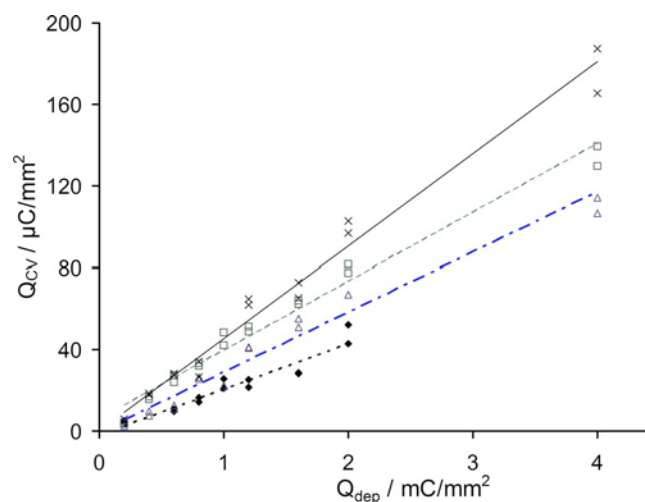


Fig. 3. Enclosed charge by both anodic and cathodic sweep in CV curve. Films deposited with different charges Q_{dep} for PEDOT:fibrinogen (\blacklozenge), PEDOT:heparin (\square), PEDOT:HA (\triangle), and PEDOT:PSS (\times). Lines shown are linear least square fits to data.

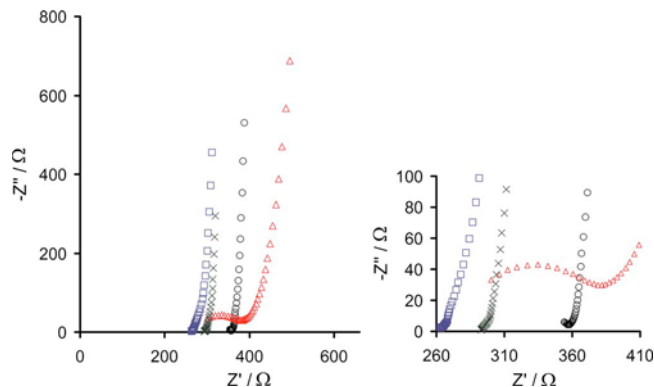


Fig. 4. Nyquist plot of PEDOT:PSS (\times), PEDOT:heparin (\square), PEDOT:HA (\circ), and PEDOT:fibrinogen (\triangle) electrodes deposited with 2 mC/mm^2 . A high frequency semicircle can be seen for PEDOT:fibrinogen and also the beginning of such a circle for PEDOT:HA.

more voltage to be applied to pass the same current. After a certain threshold was reached, the high voltage started over-oxidizing already deposited polymer and impedance increased dramatically. Maximum deposition charge for PEDOT:fibrinogen studied here was therefore 2 mC/mm^2 .

A. EIS

EIS at a sinusoidal signal E_{dc} of amplitude 0.2 V was performed in 0.1 M KCl(aq) for PEDOT:biomolecular films polymerized galvanostatically with $4 \mu\text{A}$ for 300, 500, 800, and 1000 s, respectively, and in 0.1 M NaPSS(aq) for the 800 s polymer films. From the impedance plot in Fig. 4 it can be seen that for PEDOT:heparin and PEDOT:HA, from lowest to highest frequency the impedance goes from mainly capacitive to mainly resistive, with a deviation at intermediate frequencies resembling the 45° angle of a Warburg diffusion element. The low and intermediate frequency part of the spectra is related to ion diffusion and redox capacitance in the polymer film as described by previous authors.^{11,32,33,47} The Warburg region is slightly longer for PEDOT:heparin than PEDOT:HA and PEDOT:PSS which indicates higher ionic resistance of PEDOT:heparin.

PEDOT:fibrinogen overall has the same behavior for increasing frequencies but there is also a high frequency semicircle seen ($>440 \text{ Hz}$) similar to the findings presented by Danielsson *et al.*³⁴ (2004) for PEDOT studied in bulky organic liquids and by Cui *et al.*¹⁷ (2001) for PPy doped with a silklike ProNectin F. At very high frequencies ($>2300 \text{ Hz}$) a slight semicircle can be seen also for the thicker films (more than 1 mC/mm^2) of PEDOT:HA. Apparently some processes that were not detectable for PEDOT:PSS or PEDOT:heparin have here become slow enough to be visible also in the frequency range studied here.

Comparing spectra from the same electrode in 0.1 M KCl and in 0.1 M NaPSS (Fig. 5) the general appearance is similar although the length of the Warburg-like region is increased in NaPSS. This can be interpreted as a stronger influence of diffusion related processes such as ionic conductivity in the bulkier electrolyte.³² Solution resistance in 0.1 M NaPSS is

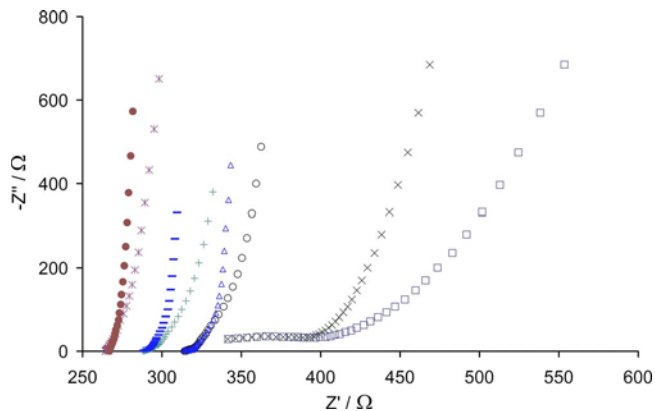


Fig. 5. Influence of electrolyte on impedance spectra. Plots show PEDOT films deposited with 1.6 mC/mm^2 and counterion HA in KCl (\bullet) and in NaPSS ($*$), NaPSS as counterion in KCl (\circ) and in NaPSS ($+$), with heparin as counterion in KCl (\triangle) and in NaPSS (\circ) and with fibrinogen as counterion in KCl (\times) and in NaPSS (\square). Spectra are arbitrary shifted on the Z' -axis for clarity.

expected to be more than double the solution resistance of 0.1 M KCl , but for comparison, the impedance plots have been shifted to the same intersection with the real axis in Fig. 4. An arbitrary shift to separate impedance of different PEDOT films was also applied to some of the curves.

B. Equivalent circuit

Through fitting an equivalent circuit to impedance spectra it is possible to extract solution resistance and study only the parameters related to the properties of the polymer films. The model suggested by Bobacka *et al.*¹¹ containing the solution resistance in series with a capacitance and the bounded Warburg diffusion element (here model 1) did not provide good fits ($\chi^2 > 0.28$) to experimental data, especially in the high frequency semicircular region, and we therefore chose the extended model suggested by Danielsson *et al.*,³⁴ here denoted model 2, containing also a capacitor in parallel with a resistance (Fig. 6). The initial values of R_S , Z_D , and C_d when fitting model 2 was however set to be the best fit for model 1. Model 2 was found to give good fit ($\chi^2 < 0.01$) to all experimental data, which was also confirmed through visual inspection (Fig. 7).

The physical interpretations of each element are as follows: the solution resistance R_S , the double layer capacitance

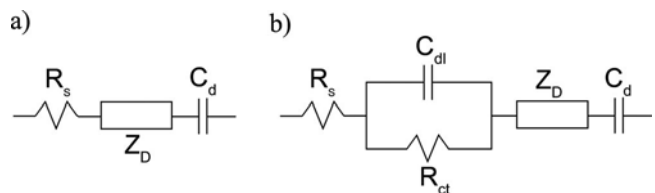


Fig. 6. (a) Model 1: equivalent circuit model containing solution resistance R_S in series with the bounded Warburg element Z_D and the electronic contribution to the bulk capacitance C_d as suggested by Bobacka *et al.* (Ref. 11) and (b) extended with the double layer capacitance C_{dl} in parallel with a charge transfer resistance R_{ct} , model 2, as suggested by Danielsson *et al.* (Ref. 34).

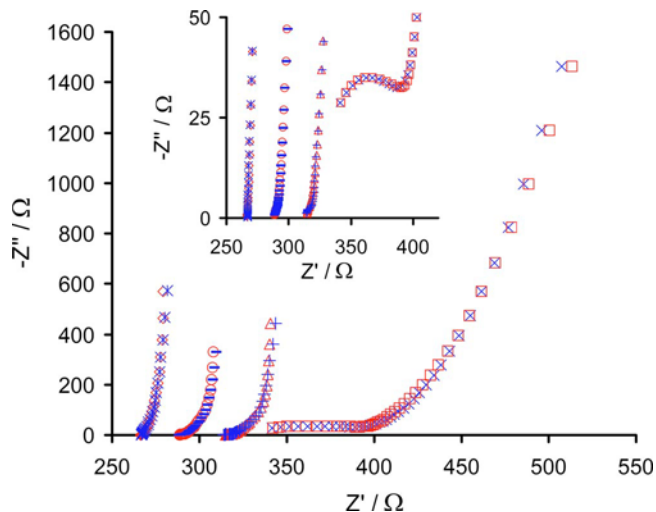


Fig. 7. Equivalent circuit compared to measurement data for PEDOT:HA measurement (*) and fit (◇), PEDOT:PSS measurement (–) and fit (○), PEDOT:heparin measurement (+) and fit (△), and PEDOT:fibrinogen measurement (×) and fit (□).

C_{dl} , the charge transfer resistance R_{ct} , and the electronic contribution to the bulk capacitance C_d . Z_D is the bounded Warburg element commonly representing diffusion within a thin layer of electrolyte.³⁵ Z_D is determined by the diffusional time constant (τ_D), diffusional pseudocapacitance (C_D), and the diffusion resistance ($R_D = \tau_D/C_D$) according to

$$Z_D = \frac{1}{Y\sqrt{j\omega}} \coth(B\sqrt{j\omega}) = \left\| Y_0 = \frac{C_D}{\sqrt{\tau_D}}, \quad B = \sqrt{\tau_D} \right\|$$

$$= \frac{\tau_D \coth\sqrt{j\omega\tau_D}}{C_D \sqrt{j\omega\tau_D}}. \quad (1)$$

Numerical values of these elements after fit to experimental data can be found in Table II. Since two measurements were made at each deposition charge the values presented are the mean of these two measurements.

C. Capacitance

C_d was found to increase proportional to deposition charge for all PEDOT films. For all materials C_D also increased with deposition charge apart for PEDOT:fibrinogen that on the contrary shows a decrease in C_D when the film grows thicker. For all thicknesses and molecules, $C_D \gg C_d$ meaning that the total interfacial capacitance $C_{tot} = 1/(1/C_D + 1/C_d)$ is dominated by the electronic contribution to the bulk redox capacitance.¹¹ As a consequence, total interfacial capacitance $C_{tot} = 1/(1/C_D + 1/C_d)$ increases linearly with increasing film thickness for all PEDOT:biomolecular composites as can be seen in Figs. 8 and 9.

Capacitance can also be calculated from cyclic voltammograms as $C_{CV} = I/\nu$, where ν is the sweep rate and I is the average of the anodic and cathodic currents at $V=0.2$ V. C_{CV} measured did follow the same linear increase with deposition charge and was in the same range as C_{tot} . The ratio

TABLE II. Elements calculated from model 2 equivalent circuit fitted to impedance spectroscopy data (3 Hz–10 kHz) and from cyclic voltammetry at sweep rate of 0.1 V/s.

Counterion	Electrolyte	Q_{dep} (mC/mm ²)	R_D (Ω)	C_D (mC)	C_d (μC)	C_{tot} (μC)	C_{CV} (μC) ^a	τ_D (s)	C_{CV}/C_{tot}
Fibrinogen	0.1M KCl	2	1310	1.25	88.3	82.3	94.8	1.69	1.15
	0.1M KCl	1.6	1380	0.698	62.4	54.5	66.5	0.642	1.22
	0.1M KCl	1	596	1.78	34.8	33.8	35.1	0.811	1.04
	0.1M KCl	0.6	259	2.60	20.8	20.7	16.5	0.618	0.797
	0.1M NaPSS	1.6	2250	0.547	52.0	47	60.3	1.16	1.28
Heparin	0.1M KCl	2	95.2	1.31	129	116	165	0.107	1.42
	0.1M KCl	1.6	65.0	1.66	134	124	143	0.104	1.15
	0.1M KCl	1	70.5	0.975	95.4	86.5	92.2	0.0630	1.07
	0.1M KCl	0.6	48.6	0.690	54.0	50.0	38.6	0.0332	0.772
	0.1M NaPSS	1.6	148	1.23	124	113	141	0.183	1.25
HA	0.1M KCl	2	69.6	2.24	107	102	115	0.154	1.13
	0.1M KCl	1.6	45.8	3.040	96.5	93.3	95.8	0.136	1.03
	0.1M KCl	1	36.6	1.75	57.1	55.2	46.2	0.0649	0.837
	0.1M KCl	0.6	51.6	1.04	34.9	33.7	24.4	0.0522	0.724
	0.1M NaPSS	1.6	240	4.65	87.3	85.7	101	1.11	1.18
PSS	0.1M KCl	2	68.1	2.26	193	177	210	0.154	1.19
	0.1M KCl	1.6	65.4	2.31	173	159	183	0.128	1.15
	0.1M KCl	1	53.8	1.03	81.3	75.3	76.4	0.0558	1.01
	0.1M KCl	0.6	70.7	0.905	63.1	59.0	53.6	0.0651	0.908
	0.1M NaPSS	1.6	174.6	1.70	156	143	183	0.288	1.28

^a C_{CV} was calculated from CV scans made immediately before impedance spectroscopy. Comparison with C_{tot} measured in NaPSS was made with CV measurements performed in NaPSS.

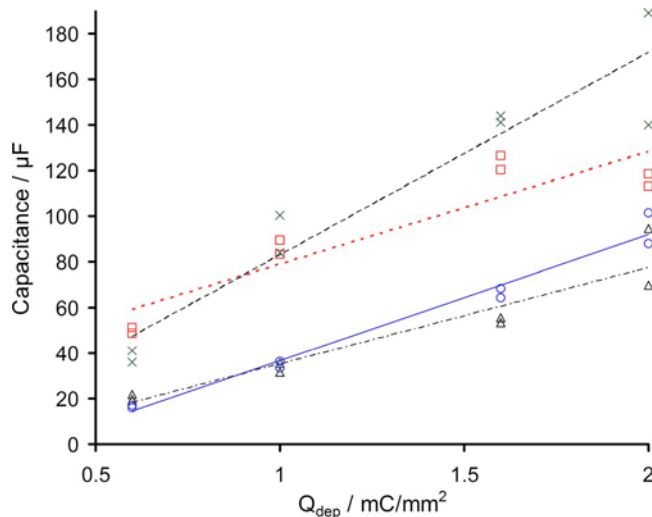


FIG. 8. Capacitance at different deposition charges Q_{dep} measured by impedance spectroscopy C_{tot} for PEDOT:fibrinogen (Δ) and PEDOT:heparin (\square) and by cyclic voltammetry C_{CV} for PEDOT:fibrinogen (\circ) and for PEDOT:heparin (\times).

$C_{\text{CV}}/C_{\text{tot}}$ was in general more than 1 for the thicker films ($Q_{\text{dep}} > 1 \text{ mC/mm}^2$) and less than 1 for $Q_{\text{dep}} \leq 1 \text{ mC/mm}^2$. C_{CV} 's larger than C_{tot} would be expected,¹¹ an effect believed to be the result of the different behaviors of the PEDOT film at a relatively low sweep rate enabling also slower redox reactions to contribute to the total current response. Considering Bobacka *et al.* studied films thicker than 0.7 mC/mm^2 , our result is still in good agreement with their measurements. They also reported $C_{\text{CV}}/C_{\text{tot}}$ ratios larger than 2 for films with restricted ion transport in the polymer film. The fact that our measurements show ratios close to 1 indicates that the PEDOT:biomolecular films has good ion transport properties in KCl electrolyte.

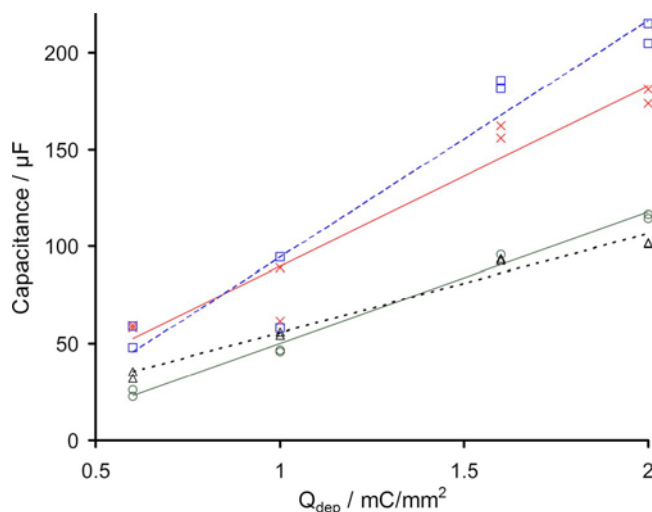


FIG. 9. C_{tot} for PEDOT:HA (Δ) and PEDOT:PSS (\times) and C_{CV} for PEDOT:HA (\circ) and for PEDOT:PSS (\square).

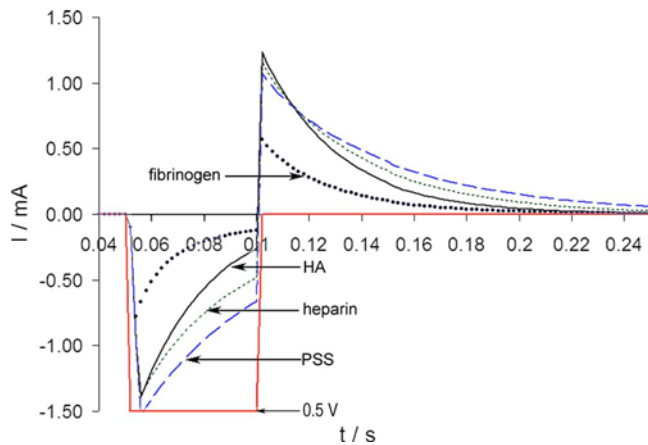


FIG. 10. Current response of electrodes deposited with 1.6 mC/mm^2 for PEDOT:fibrinogen (\bullet), PEDOT:heparin ($- -$), PEDOT:HA ($-$), and PEDOT:PSS ($- \cdot -$).

D. Resistances and τ_D

The mean R_S calculated from all 32 measurements in $0.1M$ KCl was 278Ω with standard deviation $\sigma_{R_S}=53 \Omega$ and in $0.1M$ NaPSS 565Ω , $\sigma_{R_S}=64$. As can be seen from Table II, R_D was found to be independent of film thicknesses for all combinations apart from PEDOT:fibrinogen, where a higher diffusion resistance was seen as the films grew thicker. R_D for PEDOT:fibrinogen was also found to be an order of magnitude higher than for the other materials. Diffusional time constants were in the range 0.6 – 1.7 s for PEDOT:fibrinogen and 0.03 – 0.15 s for all the other PEDOT films indicating also slower ion transport in PEDOT:fibrinogen.

E. Potentiometric measurement

As can be seen from Fig. 10, the current response to 0.5 V cathodic pulses was first a negative current in the milliamperere range during the pulse and an anodic recharging current during the subsequent 200 ms of 0 V . If current is integrated with respect to time during the 0.5 V charging pulse and compared to the charge in the anodic recharging current over the 150 ms following, the areas are approximately equal. The residual current after the 150 ms is less than $25 \mu\text{A}$ for all the PEDOT:biomolecules which is less than 2% of the maximum current during discharge. The total charge during the 150 ms discharge is as follows (the average of ten measurements for each of the two electrodes): PEDOT:heparin $21 \mu\text{C}$, PEDOT:HA $18 \mu\text{C}$, PEDOT:fibrinogen $6.5 \mu\text{C}$, and PEDOT:PSS $25 \mu\text{C}$.

F. Surface studies

Wettability of the surfaces was studied with a CAM 200 goniometer (KSV Instruments, Helsinki Finland) and static contact angles were measured at two points per sample and at least four samples of each material. From Table III it can be seen that the standard deviation between measurements was high which might indicate rather rough surfaces. SEM

TABLE III. Contact angle θ for PEDOT electrodeposited with different counterions.

Counterion	θ^a (°)	σ
PSS	44.8	10.5
HA	43.6	24.1
Heparin	19.6	6.0
Fibrinogen	46.5	27.2

^aAverage of two measurements at each sample and at least four samples for each material.

also revealed surfaces with a porous structure that increased from rather smooth in 60 000 times magnification when PSS had been used as counterion, to more porous for PEDOT:heparin and PEDOT:HA, to very rough with large pores of several 100 nm for PEDOT:fibrinogen (Fig. 11). One should bear in mind that SEM is performed on the film in its dried state and its appearance when swelled in solution might be quite different. Atomic force microscope can be used to study the film also in its swelled state⁵ but is beyond the scope of this article.

G. Toluidine blue assay and iodine-125 staining

Toluidine blue assay showed that PEDOT:heparin and PEDOT:HA probes had 9 and 12 $\mu\text{g}/\text{cm}^2$ biomolecules exposed on the surface, respectively. As stated by others²¹ not all heparin or HA incorporated in the film will be accessible to the toluidine blue but only a fraction of the actual biomolecule content will be detected by the assay. Iodine-125 stained fibrinogen should however reveal all fibrinogen incorporated in the film. Two samples (0.25 cm^2) at three different deposition charges, 90, 180, and 270 mC/cm^2 and also two samples (0.125 mm^2) at 90 mC/cm^2 were evaluated. Estimated fibrinogen content was in the range of $0.1 \mu\text{g}/\text{cm}^2$. Surprisingly, there was low correlation ($\rho=0.23$) between deposition charge and fibrinogen content. Larger surface area did however correlate with increased fibrinogen content ($\rho=0.90$) although the number of samples was small. This shows that fibrinogen is incorporated in the film but not as a counterion in the polymerization process but mainly through passive adsorption to the surface.

IV. DISCUSSION

We have shown that it is possible to electropolymerize PEDOT from EDOT solution using electrolytes based on biomolecules. The amount of polymer deposited can be controlled by the charge applied during electropolymerization and the capacitance of the polymer layer increases with increasing deposition charge. EIS data could successfully be fitted with equivalent circuit model 2 and analysis of its respective components give information of the electrochemical events in the PEDOT:biomolecular films.

The Nyquist plot together with the equivalent circuit showed that PEDOT:HA and PEDOT:heparin has an overall behavior similar to PEDOT:PSS in 0.1M KCl. The increase in τ_D with film thickness followed a linear relationship for all polymer films rather than a squared increase, which would be the case if diffusion length coincided with film thickness. As stated by previous authors the physical interpretation of this would be that the film also contains a significant amount of electrolyte which can diffuse through the porous structure of the film.^{11,18}

Ionic conductivity in electropolymerized PEDOT:PSS films has been shown to follow a two phase structure. Electrolyte filled pores in the film are interconnected with perm selective polymer aggregates implying the respective resistances of each phase are connected in series.³⁶ Ionic resistance is expected to be dominated by conductivity in the pores³² so that higher ionic conductivity would correlate with greater porosity. Solution resistance in 0.1M NaPSS is approximately double the resistance of 0.1M KCl which should yield a higher ionic resistance in the former electrolyte due to lower conductivity in the pores. When evaluating ionic conductivity for the different PEDOT materials we did however see different behaviors from all three cases. For PEDOT:HA, R_D in KCl was lower for than for any of the other materials which would yield a film of high porosity and hence good ionic conductivity. Despite this, ionic resistance increased more than five times when changing to NaPSS electrolyte. Corresponding $R_D(\text{NaPSS})/R_D(\text{KCl})$ ratio for PEDOT:heparin was 2.3 and for PEDOT:PSS was 2.7. A possible explanation could be that the perm selective phase is instead limiting for PEDOT:HA in the bulkier electrolyte, and PSS^- cannot enter the PEDOT:HA polymer phase. For PEDOT:fibrinogen, equivalent circuits showed R_D five to ten

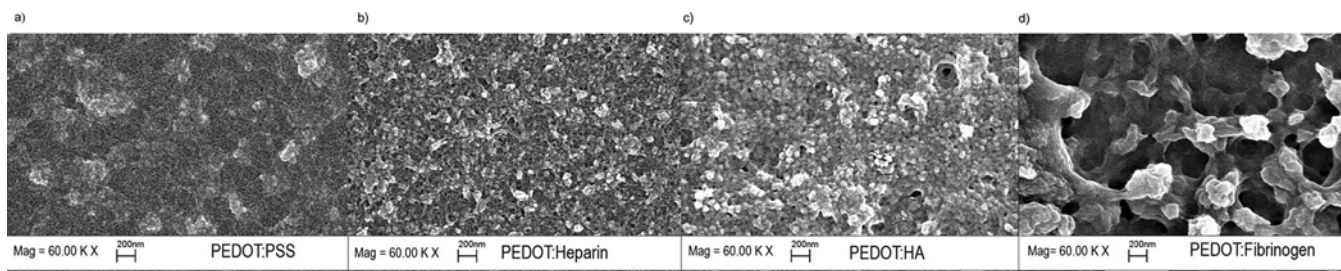


FIG. 11. Scanning electron micrographs of PEDOT electrodeposited on gold on glass substrates with counterion (a) PSS, (b) heparin, (c) HA, and (d) fibrinogen.

times greater than for the other films and hence low ionic conductivity of the PEDOT film. SEM on the other hand showed a very open morphology and also the change to a bulkier electrolyte did not affect R_D differently than for the other films [$R_D(\text{NaPSS})/R_D(\text{KCl})$ was 1.6]. In this case, ionic conductivity seems to be limited by the polymer phase irrespective of electrolyte.

PEDOT:fibrinogen also has a different impedance behaviors in other aspects apart from the high values of R_D . C_D decreases with growing film thickness unlike for the other counterions and CV scans shows a lower yield of electroactive polymer from polymerization. The Nyquist plot has a pronounced high frequency semi circle indicating slow charge transfer over the polymer/electrolyte interface.

The probable interpretation is that a significant amount of a non conducting or at least low conducting material is built into the PEDOT:fibrinogen film. If a nonconducting phase was also incorporated in the polymer; electrolyte diffusion in pores could still be large while the insulating components would limit diffusion between pores, giving low ionic conductivity of the film. The insulating phase would limit the available sites for charge transfer and thereby increase resistance and decrease the amount of polymer that can contribute to the redox capacitance. Nonconducting film components could be caused by a higher potential during polymerization of PEDOT:fibrinogen, which could contribute to undesired side reactions. However the polymerization potential in EDOT:HA solutions was of the same magnitude and also the amount of side reactions is expected to be low for voltages less than 1.05 V,¹⁶ so this could not be the explanation. We believe instead that the reason is a competitive adsorption of fibrinogen to the surface in parallel with the polymerization process. This is also in accordance with results from iodine-125 staining showing no correlation between polymerization time and the amount of incorporated fibrinogen.

For implanted stimulating electrodes it is of great importance to deliver charge pulses into tissue using reversible effects for charge transfer and keep irreversible Faradaic reactions at a minimum. For most electrodes (not valence change electrodes) the main mechanism available for this is the capacitive charging and discharging of the Helmholtz double layer. High capacitance of the electrode/electrolyte interface is therefore desirable and will be the main limiting factor for electrode miniaturization. There is no absolute charge delivery threshold that must be reached for a material to be considered for stimulating electrodes but the required charge varies greatly with application. In general it can however be said that miniaturization of electrodes opens up for less invasive implants and more individual communication channels which, in turn, increases selectivity of both recording and stimulation. In this respect, miniaturization of electrodes will be the step needed to make more exquisite neuroprosthetic applications possible.

Required charge to elicit a desired neural response is not a well known fixed quantity but depends on a large set of parameters like proximity to the target neural structure, stimulation frequency, if cathode or anode pulse is applied

first, desired effect of stimulation and also properties of the neural tissue itself. Neuroprosthetics includes applications with stimulation of peripheral nerves, cranial nerves, as well as direct stimulation of cortical neurons and the prerequisites for these applications vary widely.

To give some figures of merit Cogan *et al.*¹⁰ suggested that small area electrodes ($<2000 \mu\text{m}^2$) should be able to deliver at least $5 \mu\text{C}/\text{mm}^2$ to be considered for neuroprosthetics concerning stimulation in the central nervous system, while in earlier literature statements of desired charge densities as high as $100 \mu\text{C}/\text{mm}^2$ can be found.³⁷ In the peripheral nervous system, several different scenarios exist. Implanted electrodes can be placed both outside the nerve trunk, as with cuff electrodes or intrafascicularly. Through intrafascicular electrodes, stimulation at lower threshold charges can be achieved and higher selectivity can also be expected, assuming electrodes can be made small enough to allow complete electrode array systems to be implanted. Placing electrodes on a cuff makes it possible to use larger electrode surfaces than for penetrating structures, which must be thin not to create harmful tissue displacement within the nerve. On the other hand, stimulation charge must be higher to transfer charge also through the epineural sheath. Branner *et al.*³⁸ compared cuff electrodes and intrafascicular electrodes through stimulating the cat sciatic nerve and according to their findings, the mean charge needed to produce maximum recruitment response for intrafascicular platinum electrodes of area 0.005 mm^2 was 6.3 nC ($1.26 \mu\text{C}/\text{mm}^2$) and also reported that the stimulation currents needed were "an order of magnitude smaller" than those evoked with the cuff electrode. In a study of phosphene threshold for a blind volunteer stimulated with a cuff electrode round the optic nerve, it was observed that depending on frequency and pulse duration, thresholds were within $2.5\text{--}50 \text{ nC}$ delivered from electrodes of contact area 0.2 mm^2 ($0.0125\text{--}0.25 \mu\text{C}/\text{mm}^2$).³⁹

The retina implant is a demanding application with respects to charge delivery considering that functionality of a visual prosthetics is depending on a high number of pixels, at the very least a 25×25 matrix, to be fitted into a restricted space.⁴⁰⁻⁴² At the same time stimulation charge must be high enough to traverse the retina and reach spiral ganglions giving that charge delivery requirements sets a lower limit for electrode density and thereby pixel density of the vision system. Reasonable size for a retinal implant is around $3 \times 3 \text{ mm}^2$ (the fovea diameter is $\sim 1.5 \text{ mm}$) so 625 electrodes could be fit into the implant if electrode diameter is less than $100 \mu\text{m}$. Keeping in mind that the diameter of ganglion cells is in the range $10\text{--}20 \mu\text{m}$,⁴³ diameters in the range $25\text{--}100 \mu\text{m}$ seem reasonable even though the smaller diameter would be preferred for higher resolution.⁴⁴ Thresholds for epiretinal stimulation with large surface electrodes ($>500 \mu\text{m}$ diameter) has been determined to be less than $3.5 \mu\text{C}/\text{mm}^2$.⁴⁵ An *in vitro* method on chicken retina suggests subretinal threshold charges in the range $0.4\text{--}0.7 \text{ nC}$ from very small electrodes ($10 \mu\text{m}$ in diameter) which yields a charge density of $5\text{--}9 \mu\text{C}/\text{mm}^2$.⁴⁶

From potentiometric measurements we have shown that we can deliver charges in the range 6.5–21 $\mu\text{C}/\text{mm}^2$ from our PEDOT electrodes deposited with at least 1.6 mC/mm^2 . This is not an empirically determined maximum charge delivery capacity but rather an estimate of how much charge we actually deliver if kept within reasonably safe polarization boundaries. Previous articles on the stability of PEDOT have shown that it can be polarized at 0.4 V for 16 h and still keep major part of its electroactivity.²⁴ Pulse shape, frequency, and duration as well as the environment in which the electrode is placed will influence its electrochemical stability and to give a good estimate on maximum charge delivery, long term stimulation, and subsequent stability evaluation should be performed but is beyond the scope of this article. The charge delivered from our 1.6 mC/mm^2 PEDOT films is in the range of the charge per area required for the applications described above. Higher deposition charges can be used to build thicker polymer films and get higher charge delivery if required.⁴ PEDOT films with charges as high as 40 μC has successfully been grown³³ which if normalized with surface area, yields a deposition charge of 32 mC/mm^2 . One should keep in mind that they use micro-sized probes and more than double current density (0.5 mA/cm^2) and also the choice of counterion will influence the growth pattern of the polymer. It is however a good indication of that PEDOT films can be grown quite thick and still keep a rather open morphology. PEDOT layers deposited electrochemically from monomer solution can also be made more permeable to the electrolyte as shown with hydrogel electrodes.⁹ This would further increase the electrolyte contact and the amount of polymer that can contribute in charge delivery and should bring us closer to the 0.34 mC/mm^2 reported by Nyberg *et al.* (2002).⁴

V. CONCLUSIONS

The charged biomolecules heparin and HA can be used as counterions in the electrochemical deposition of PEDOT from aqueous EDOT solution. PEDOT can also be electropolymerized in the presence of fibrinogen, but it is plausible that fibrinogen itself does not take part in the polymerization process and is passively adsorbed to the surface in parallel with the polymerization process. The choice of counterion influences both the electrochemical properties and microstructure of the resulting PEDOT film significantly. Heparin and HA give films similar to PEDOT:PSS while PEDOT deposited from fibrinogen solution have lower conductivity. The highest yield of electroactive polymer was given by PEDOT:heparin which showed polymerization potential almost as low as PEDOT:PSS. Even if PEDOT:HA showed the highest ionic conductivity in KCl it appeared much more resistive in the bulkier electrolyte. We therefore propose PEDOT:heparin as an interesting alternative to PEDOT:PSS for implanted electrodes. The hydrophilic properties provided by the heparin might also enhance neuron ingrowth toward the electrode. Further experiments on biocompatibility, activity of incorporated heparin and stability of the PEDOT:heparin complex will be the focus of future studies.

ACKNOWLEDGMENTS

The authors thank Pentti Tengvall, Linköping University, and Tobias Nyberg at the Royal Institute of Technology for helpful discussions and Shimelis Admassie, Addis Ababa University, and Christian Ulrich, Linköping University for experimental assistance. This work was also supported by the Strategic Research Foundation SSF through OBOE, the Center of Organic Bioelectronics.

- ¹S. B. Brummer and M. J. Turner, *Bioelectrochem. Bioenerg.* **2**, 13 (1975).
- ²L. A. Geddes and R. Roeder, *Ann. Biomed. Eng.* **31**, 879 (2003).
- ³C. Veraart, W. M. Grill, and J. T. Mortimer, *IEEE Trans. Biomed. Eng.* **40**, 640 (1993).
- ⁴T. Nyberg, O. Inganäs, and H. Jerregard, *Biomed. Microdevices* **4**, 43 (2002).
- ⁵T. Nyberg, A. Shimada, and K. Torimitsu, *J. Neurosci. Methods* **160**, 16 (2007).
- ⁶Y. H. Xiao, D. C. Martin, X. Y. Cui, and M. Shenai, *Appl. Biochem. Biotechnol.* **128**, 117 (2006).
- ⁷J. Y. Yang and D. C. Martin, *Sens. Actuators, A* **113**, 204 (2004).
- ⁸K. A. Ludwig, J. D. Uram, J. Y. Yang, D. C. Martin, and D. R. Kipke, *J. Neural Eng.* **3**, 59 (2006).
- ⁹S. Ghosh and O. Inganäs, *Adv. Mater. (Weinheim, Ger.)* **11**, 1214 (1999).
- ¹⁰S. F. Cogan, P. R. Troyk, J. Ehrlich, T. D. Plante, and D. E. Detlefsen, *IEEE Trans. Biomed. Eng.* **53**, 327 (2006).
- ¹¹J. Bobacka, A. Lewenstam, and A. Ivaska, *J. Electroanal. Chem.* **489**, 17 (2000).
- ¹²A. Lima, P. Schottland, S. Sadki, and C. Chevrot, *Synth. Met.* **93**, 33 (1998).
- ¹³D. Kim, S. Richardson-Burns, J. Hendricks, C. Sequera, and D. Martin, *Adv. Funct. Mater.* **17**, 79 (2007).
- ¹⁴N. Sakmeche, S. Aeyach, J. J. Aaron, M. Jouini, J. C. Lacroix, and P. C. Lacaze, *Langmuir* **15**, 2566 (1999).
- ¹⁵R. Schweiss, J. F. Lubben, D. Johannsmann, and W. Knoll, *Electrochim. Acta* **50**, 2849 (2005).
- ¹⁶L. Pigani, A. Heras, A. Colina, R. Seeber, and J. Lopez-Palacios, *Electrochim. Commun.* **6**, 1192 (2004).
- ¹⁷X. Y. Cui, V. A. Lee, Y. Raphael, J. A. Wiler, J. F. Hetke, D. J. Anderson, and D. C. Martin, *J. Biomed. Mater. Res.* **56**, 261 (2001).
- ¹⁸X. Y. Cui and D. C. Martin, *Sens. Actuators B* **89**, 92 (2003).
- ¹⁹L. Cen, K. G. Neoh, and E. T. Kang, *Langmuir* **18**, 8633 (2002).
- ²⁰B. Garner, A. J. Hodgson, G. G. Wallace, and P. A. Underwood, *J. Mater. Sci.: Mater. Med.* **10**, 19 (1999).
- ²¹D. Zhou, C. O. Too, and G. G. Wallace, *React. Funct. Polym.* **39**, 19 (1999).
- ²²B. Garner, A. Georgevich, A. J. Hodgson, L. Liu, and G. G. Wallace, *J. Biomed. Mater. Res.* **44**, 121 (1999).
- ²³J. H. Collier, J. P. Camp, T. W. Hudson, and C. E. Schmidt, *J. Biomed. Mater. Res.* **50**, 574 (2000).
- ²⁴H. Yamato, M. Ohwa, and W. Wernet, *J. Electroanal. Chem.* **397**, 163 (1995).
- ²⁵P. K. Smith, A. K. Mallia, and G. T. Hermanson, *Anal. Biochem.* **109**, 466 (1980).
- ²⁶I. K. Kang, O. H. Kwon, Y. M. Lee, and Y. K. Sung, *Biomaterials* **17**, 841 (1996).
- ²⁷N. Blumenkrantz, *Clin. Chem.* **3**, 696 (1957).
- ²⁸P. Cosman and S. G. Roscoe, *Langmuir* **20**, 1711 (2004).
- ²⁹P. Bernabeu and A. Caprani, *Biomaterials* **11**, 258 (1990).
- ³⁰K. B. Lewis and B. D. Ratner, *Colloids Surf., B* **7**, 259 (1996).
- ³¹R. D. Meyer, S. E. Cogan, T. H. Nguyen, and R. D. Rauh, *IEEE Trans. Neural Syst. Rehabil. Eng.* **9**, 2 (2001).
- ³²G. C. Li and P. G. Pickup, *Phys. Chem. Chem. Phys.* **2**, 1255 (2000).
- ³³Y. H. Xiao, X. Y. Cui, and D. C. Martin, *J. Electroanal. Chem.* **573**, 43 (2004).
- ³⁴P. Danielsson, J. Bobacka, and A. Ivaska, *J. Solid State Electrochem.* **8**, 809 (2004).
- ³⁵*Impedance Spectroscopy*, 2nd ed., edited by E. Barsoukov and J. R. Macdonald (Wiley, New York, 2005).
- ³⁶X. M. Ren and P. G. Pickup, *J. Electroanal. Chem.* **396**, 359 (1995).

- ³⁷T. L. Rose, E. M. Kelliher, and L. S. Robblee, *J. Neurosci. Methods* **12**, 181 (1985).
- ³⁸A. Branner, R. B. Stein, and R. A. Normann, *J. Neurophysiol.* **85**, 1585 (2001).
- ³⁹C. Veraart, J. T. Mortimer, J. Delbeke, D. Pins, G. Michaux, A. Vanlierde, S. Parrini, and M. C. Wanet-Defalque, *Brain Res.* **813**, 181 (1998).
- ⁴⁰K. Cha, K. W. Horch, and R. A. Normann, *Vision Res.* **32**, 1367 (1992).
- ⁴¹R. W. Thompson, Jr., G. D. Barnett, M. S. Humayun, and G. Dagnelie, *Invest. Ophthalmol. Visual Sci.* **44**, 5035 (2003).
- ⁴²H. G. Sachs and V. P. Gabel, *Albrecht von Graefes Arch. Klin. Exp. Ophthalmol.* **242**, 717 (2004).
- ⁴³M. S. Humayun, E. de Juan, J. D. Weiland, G. Dagnelie, S. Katona, R. Greenberg, and S. Suzuki, *Vision Res.* **39**, 2569 (1999).
- ⁴⁴J. D. Loudin, D. M. Simanovskii, K. Vijayraghavan, C. K. Sramek, A. F. Butterwick, P. Huie, G. Y. McLean, and D. V. Palanker, *J. Neural Eng.* **4**, S72 (2007).
- ⁴⁵M. S. Humayun *et al.*, *Vision Res.* **43**, 2573 (2003).
- ⁴⁶A. Stett, W. Barth, S. Weiss, H. Haemmerle, and E. Zrenner, *Vision Res.* **40**, 1785 (2000).
- ⁴⁷M. Lefebvre, Z. G. Qi, D. Rana, and P. G. Pickup, *Chem. Mater.* **11**, 262 (1999).